

Corrosion of a unidirectionally solidified $\text{Al}_2\text{O}_3/\text{YAG}$ eutectic composite in a combustion environment

Akihiko Otsuka^{a,*}, Yoshiharu Waku^b, Ryohei Tanaka^c

^a Organic Coating and Composite Products Department, Nisshin Steel Co., Ltd., 7-1 Kohya-Shinmachi, Ichikawa-City, Chiba-pref. 272-0011, Japan

^b Ube Industries, Ltd., Japan

^c Japan Ultra-high Temperature Materials Research Institute, Japan

Available online 11 February 2005

Abstract

Owing to their remarkable higher creep resistance, some oxides eutectic composites those fabricated by unidirectional solidification are prime candidates for structural components used in a severe corrosive environment at high temperatures. In this paper, the possibility of an $\text{Al}_2\text{O}_3/\text{YAG}$ eutectic composite for high-temperature application, where the materials would be exposed to combustion gases, was investigated. The $\text{Al}_2\text{O}_3/\text{YAG}$ eutectic composite was stable at 1700 °C in an atmosphere of oxygen/water vapor ($\text{O}_2/\text{H}_2\text{O}$), showing only slight changes in microstructure, volume and flexural strength after an exposure for 200 h. Thus, $\text{Al}_2\text{O}_3/\text{YAG}$ eutectic composite is among the most promising ceramics for structural applications at high temperatures.

© 2004 Elsevier Ltd. All rights reserved.

Keywords: Composites; Corrosion; Engine components; Microstructure-final

1. Introduction

In order to improve the reliability of ceramics, some new material systems have been developed, which have the ability to produce microstructures in situ with unique micromorphology that allow toughening mechanisms to take place. These self-reinforced ceramics can be formed by (i) growth from the liquid phase (e.g., $\text{Si}_3\text{N}_4\text{Al}_2\text{O}_3$ and mullite);^{1–3} (ii) by decomposition of single solid solution (e.g., $\text{AlN}-\text{SiC}$);⁴ and by (iii) simultaneous crystallization of more than one solid from a eutectic composition liquid (e.g., directionally solidified oxide eutectic composites those we call as melt-growth-composites, MGCs).⁵ In all cases, the initial composition forms a liquid or solid solution with a different morphology. The preferred crack propagation along interface boundaries makes them more flaw-tolerant than monoliths. The availability of common raw materials, lower production cost than that of the fiber composites, and good controllability of phase morphology are also their advantages.

The major attractive feature of MGCs lies in improvement of the creep property at high temperatures. Polycrystal ceramics are usually composed of many grains with different orientations. A grain boundary has excess energy, therefore, grain growth and grain boundary diffusion creep will easily progress at high temperatures. In the extreme case, superplasticity occurs due to grain boundary sliding if the ceramics contain a widely distributed non-crystalline grain boundary film. In contrast, MGCs have neither grain boundaries nor colonies as can be seen in Fig. 1.⁶ This unique microstructure is grown by the unidirectional solidification from ceramic melts with a eutectic composition which minimizes the free energy at the interface, resulting in single crystal phases entangled with each other.

In addition, locally distributed thermal residual stresses develop in the eutectic composite upon cooling from the solidification processing temperature as a result of the mismatch in thermal expansion coefficients between both phases (in the case of binary eutectic composite). The compressive residual stresses if they were formed in the more brittle phase of the eutectic composite will contribute actively to increase its strength. Because, failure is likely to start in the weaker

* Corresponding author. Tel.: +81 47 328 8255; fax: +81 47 328 8218.
E-mail address: n04403@nisshin-steel.co.jp (A. Otsuka).

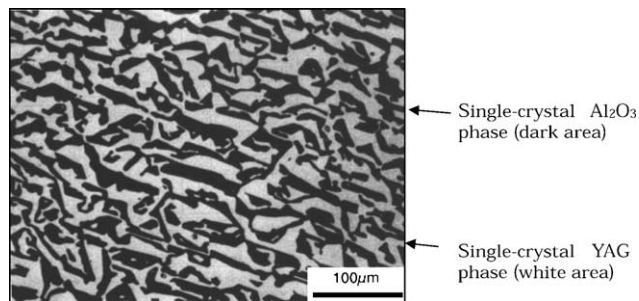


Fig. 1. Microstructure of a unidirectionally solidified $\text{Al}_2\text{O}_3/\text{YAG}$ eutectic composite (melt growth composite, MGC).

phase but this requires overcome the compressive residual stresses.

On the other hands, oxide ceramics have been widely used owing to their environmental stability. However, the chemical property data of the oxide eutectic composites being formed the anisotropic residual thermostresses locally, needed to predict criteria for corrosion, are less available in the literature. Environmental resistivity, the ability to withstand high-operating temperatures, atmospheres and/or attack by corrosive melts, is an important property of materials for practical use. In this study, the stability of the $\text{Al}_2\text{O}_3/\text{Y}_3\text{Al}_5\text{O}_{12}$ (YAG) binary MGC in water vapor at 1700°C was investigated. The stability in combustion field at 1500°C was also investigated.

2. Experimental procedure

The MGC material ($\text{Al}_2\text{O}_3/\text{YAG}$ eutectic composite) used in this work was supplied from Ube Industries Ltd., Japan. It was fabricated by melting the mixture powder of $\text{Al}_2\text{O}_3/\text{Y}_2\text{O}_3 = 0.82/0.18$ in mole ratio, and solidifying directionally in a molybdenum crucible using a Bridgman technique (the growth rate: 5 mm h^{-1}) with approximately 40 mm diameter and 70 mm long. The samples for the corrosion test were cut into rectangular solid of bars ($3\text{ mm} \times 4\text{ mm} \times 40\text{ mm}$) and plates ($10\text{ mm} \times 10\text{ mm} \times 1\text{ mm}$), and all of the surface were polished to a $6\text{-}\mu\text{m}$ finish, and ultrasonically cleaned in pure analytical grade ethanol. Typical microstructure of the $\text{Al}_2\text{O}_3/\text{YAG}$ (0.52/0.48 in volume ratio) eutectic composite shows the two single crystal phases complexly interpenetrated without colony structures and fibers as in conventional directionally solidified materials (as in Fig. 1).

Corrosion tests in wet- O_2 gas were conducted up to 200 h at 1700°C in a horizontal tube furnace equipped with an Al_2O_3 tube of 99.8% purity. The bar samples were placed on high purity Al_2O_3 setters supporting the pinpoints near both edges of the sample in order to expose all of the sample surface. The sample temperature was monitored with a Pt–20% Rh thermocouple placed within 10 mm apart from the sample. The heating rate from room temperature to the test temperature of 1700°C was 250°C h^{-1} . The Al_2O_3 tube and the setter had been preheated at 1700°C for 50 h passing the wet- O_2 gas before the use for the corrosion tests.

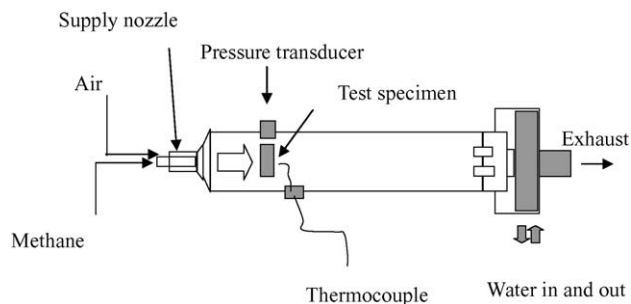


Fig. 2. Schematic drawing of a burner rig test.

The corrosive atmosphere was $\text{H}_2\text{O}: 5.0 \times 10^4\text{ Pa}$ and $\text{O}_2: 5.0 \times 10^4\text{ Pa}$ under atmospheric pressure. The gas flow rate was $3.3 \times 10^{-6}\text{ m}^3\text{ s}^{-1}$ in total. Water vapor was introduced into the oxygen stream using a saturator where oxygen was bubbling through deionized water held at 82°C .

In general, experiments of an alumina sample exposure to the wet atmospheres may be limited by mullite formation at the high end of the temperature range below 1500°C .⁸ Volatile Si–O–H species are often carried from the fused quartz tube to the alumina sample surface where mullite is nucleated. In this study, therefore, the components of the furnace where hot water vapor passing was made with high-purity alumina only, so that the Si–O–H contamination could be prevented. Mullite was not observed at any exposure temperatures up to upper limit temperature of the furnace (1700°C) in this study.

After the corrosion experiments, the weight and volume changes were measured. The three-point bending test of the corroded samples was made at a cross-head speed of 0.5 mm min^{-1} . Most of the data were averaged ones of three to four values. scanning electron microscopic (SEM) and electron microprobe Analyses (EPMA) were made to observe the microstructures and to study their chemistry. X-ray diffraction (XRD) was also used to determine the phase composition. Commercially available sintered polycrystalline Al_2O_3 (SSA-S; Nikkato Co., Japan) was also tested for comparison.

The burner rig test was conducted for examination of the effect of combustion gases including CO, CO_2 , H_2 and H_2O , on the sample recession. Fig. 2 shows a schematic of the high-pressure burner rig configuration. This burner rig was originally developed for an investigation of CH_4 combustion at high-pressures. The sequence of CH_4 combustion such as ignition of fuel gas, pressure controlling during combustion, extinguishment and forced cooling by air, is accomplished using a computer-tip-based digital data acquisition system. The ceramic samples exposed by this burner rig often resulted in crack because of its poor thermal shock resistivity, therefore, the slight change at the sample surface caused by the attack of the combustion products (i.e., radicals) was mainly investigated.

Air and CH_4 are supplied from gas cylinders to this burner rig. CH_4 is supplied through the inner nozzle of a coaxial

injector, air is fed through the outer one and ignited by a spark plug. The sample holder is made of type 430 stainless steel, inserted perpendicularly to the gas stream. Therefore, the maximum sample exposure time is limited up to 30 min because of heavy oxidation of the sample folder. The polished sample plate (10 mm × 10 mm × 1 mm) is attached to the sample folder holding the edges by two sets of screws (type 430 stainless steel) putting between thin Al₂O₃ plates (setter). A Pt–Pt13Rh (type R) thermocouple probe measured the center-line gas temperature 20–30 mm behind the sample, and the test was conducted at a temperature of about 1500 °C.

To simulate the range of gas turbine conditions, the primary test parameters used are sample temperatures of 1500 °C, pressures of 10 atm (1 atm = 0.1 MPa), gas flow velocities of 3.2 m s⁻¹, and the rich-burn ($\phi = 1.3$) or the lean-burn ($\phi = 0.9$) fuel-to-air ratios. Velocity of gas across the sample is calculated from the ideal gas law, given the cross-sectioned area at the test section. Reynold's number of the CH₄ and air flow at the outlet of the injector were 1000–2000, so the flows are laminar. The sample is heated at testing temperature within a minute, and quenched rapidly by the high-pressure air after the exposure of combustion gas.

The samples exposed to the burner rig at 1500 °C are characterized by X-ray diffraction analysis (θ – 2θ scans) with a Cu K α X-ray source (M18X, MAC Science, Japan), scanning electron microscopy and X-ray photoelectron spectroscopy with a Mg K α X-ray source (1600S, PHI).

3. Results and discussion

3.1. Stability of Al₂O₃/YAG eutectic composite in O₂/H₂O at 1700 °C

Fig. 3 shows the mass changes after an exposure to the 50% O₂/50% H₂O atmosphere (1 atm) at 1700 °C. The sintered polycrystalline Al₂O₃ showed a slight mass loss, while the Al₂O₃/YAG eutectic composite showed a slight mass gain. This suggests that the extensive vaporization did not occur. On the other hand, the mass loss of the sintered polycrys-

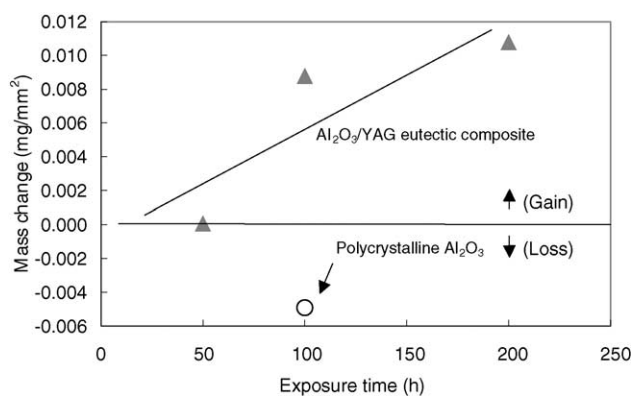


Fig. 3. Mass changes of the tested samples after exposure in O₂/H₂O at 1700 °C for 100–200 h.

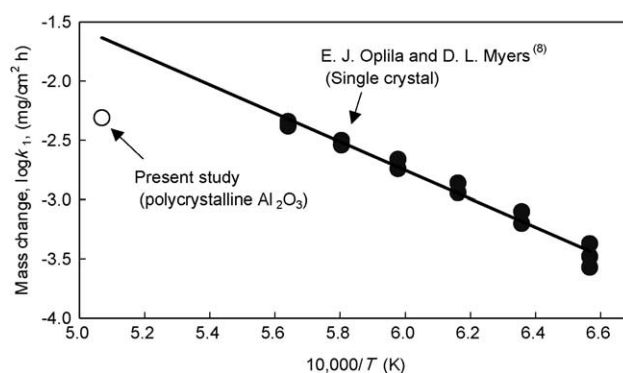
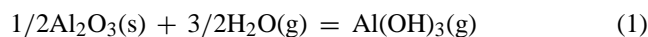


Fig. 4. Comparison of measured weight loss rates for Al₂O₃ in 0.5 atm O₂/0.5 atm H₂O.

talline Al₂O₃ indicates the formation of gaseous hydroxide. These results are published elsewhere,⁷ but are included here for completeness.

In previous work by Opila,⁸ it has been clearly demonstrated that exposure sapphire in 50% O₂/50% H₂O at temperatures exceeding 1300 °C led to the formation of Al(OH)₃(g). The volatilization of alumina to form Al(OH)₃(g) is limited by transport of this species outward through a gaseous laminar boundary layer. The reaction involved is as follows:



The measured mass-loss rate of the polycrystal Al₂O₃ in this study are shown in Fig. 4 comparing with the Opila's data. The measured mass loss rate in this study is smaller than that of Opila's data. A possible explanation for this different result may be the difference in gas velocities (1.4 mm s⁻¹ in this study and 44 mm s⁻¹ in Opila's study), because the thickness of the gaseous laminar layer is a function of the gas velocity.

On the other hand, the X-ray diffraction patterns of the Al₂O₃/YAG eutectic composite after exposure O₂/H₂O at 1700 °C for 200 h showed no peaks nor background increase associate with hydroxide and/or amorphous phase formation. These XRD results contradict with that of mass gain for the Al₂O₃/YAG eutectic composite after exposure to wet-O₂ gas. The XRD pattern reflects mainly the re-crystallized surface of the sample, while mass gain caused by interstitial diffusion of OH ions and/or the product formation (i.e., hydroxide) may take place inside of the specimen.

The question remains why the exposure of the Al₂O₃/YAG eutectic composite in wet-O₂ resulted in mass gain while polycrystalline Al₂O₃ resulted in mass loss. The explanation of this different behavior is controversial. Currently, it is thought to be related to the lower mobility of OH ions and/or H₂O molecules through the lattice of the Al₂O₃/YAG eutectic composite where compressive residual stresses are present. The thermal expansion coefficient of alumina and YAG are 5.8 × 10⁻⁶ K⁻¹ and 6.9 × 10⁻⁶ K⁻¹, respectively. Therefore, the alumina may be in compression in the Al₂O₃/YAG eutectic composite and in tension in the YAG. Taking into

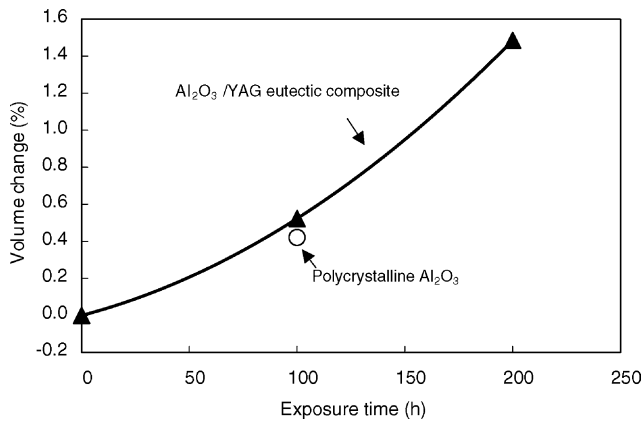


Fig. 5. Volume change as a function of exposure time.

account the higher stability of Y_2O_3 than Al_2O_3 in wet- O_2 at high temperatures,⁹ therefore, the YAG is considered to be also more stable than Al_2O_3 . Since the diffusion of OH ions and/or H_2O molecules into lattice results in strain of lattice, consequently the reaction rate of the corrosion by water vapor could be decreased by the presence of the compressive residual stresses in alumina. On contrary, OH ions and/or H_2O molecules will easy to diffuse in YAG phase where tensional stresses are presence. Thus, diffused O–H chemical species are considered to increase the weight of the exposed samples in wet atmospheres.

Diffusion of O–H chemical species results in strain of lattice. Consequently, the sample volume is changed after exposure to wet atmospheres. The changes in the sample volume after the exposure in wet- O_2 are shown in Fig. 5. The slight volume changes were encountered for the Al_2O_3 /YAG eutectic composite and the sintered polycrystalline Al_2O_3 . Similar results of the morphology changes by water-vapor attack on alumina and Al_2O_3 /YAG eutectic have been described in previous reports.^{10–12} Grain boundary etching of polycrystalline Al_2O_3 has been reported by Tai and Watanabe,¹⁰ and localized thermal grooving has been reported by Naoufai et al.¹¹ These studies show that Al_2O_3 and Al_2O_3 /YAG eutectic composite are expected to be highly stable in pure-oxygen environments. At elevated temperatures in H_2O -containing environments, Al_2O_3 and YAG decompose into gaseous species, $Al_xO_yH_z$ via several routes in the grain boundary region on

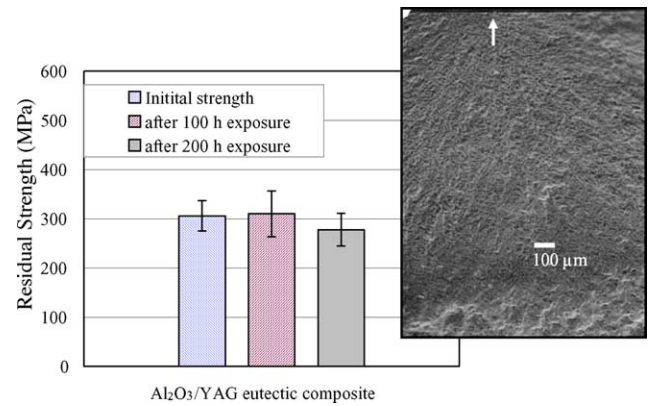


Fig. 7. Room temperature flexural strength of the Al_2O_3 /YAG eutectic composite after exposure for 100–200 h at 1700 °C in wet- O_2 . Superimposed photo is showing the fracture origin for the flexural tested sample (radial crack lines are pointing to origin).

the exposed surface or interface between Al_2O_3 and YAG. Then, these decompositions consequently cause boundary etching or localized thermal grooving on the surface of the corroded samples. In addition, segregation of internal impurities on the surface of single-crystal Al_2O_3 may occur.¹²

This work shows basically good agreement with these reports. Fig. 6 illustrates the changes in surface morphologies between the intact Al_2O_3 /YAG eutectic composite and the exposed sample to the O_2 / H_2O atmosphere for 100 h at 1700 °C. The slight thermal swelling can be observed after the exposition.

The exposed test bars of Al_2O_3 /YAG were applied to mechanical tests at room temperature, to evaluate the effects of high-temperature exposure on residual strengths of the corroded specimens. The flexural strength of the Al_2O_3 /YAG eutectic composite is almost constant after the O_2 / H_2O exposures at 1700 °C as shown in Fig. 7. The origin of fracture is the surface of the sample as can be seen in superimposed figure in Fig. 7. However, the defects of the surface, such as corrosion pits near the origin of fracture are not observed. Taking into account the almost constant fracture strengths, therefore, the surface corrosion is not the major cause of fracture in this case.

Typically, the rare formation of the cavities (Fig. 8; about 400 μm in diameter) was observed on the Al_2O_3 /YAG eutec-

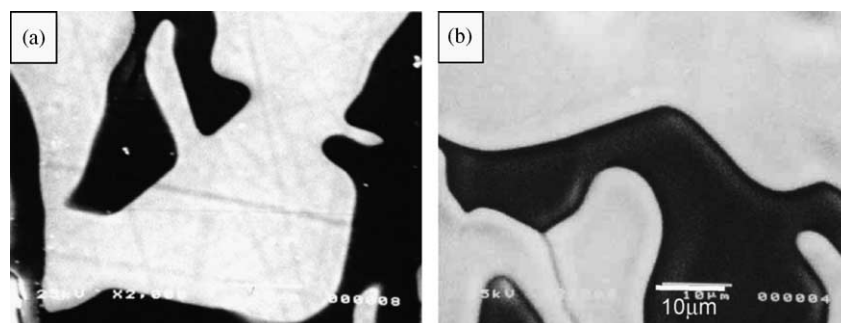


Fig. 6. SEM micrographs of the Al_2O_3 /YAG eutectic composite (a) before and (b) after exposure in O_2 / H_2O at 1700 °C for 100 h.

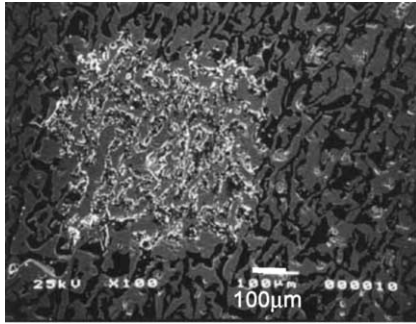


Fig. 8. Micro-cavity rarely formed by O_2/H_2O corrosion of the Al_2O_3/YAG eutectic composite.

tic composite surface corroded by wet- O_2 . Thus, reason why the cavity formation rarely encountered is considered due to the swellings of Al_2O_3 and YAG phases. The volume change in the Al_2O_3 and YAG phases must cause localized stress at the interface between these phases and lead to chippings at the stress concentrated areas on the sample surface. Such areas must become an origin of fracture. However, the stresses will be released in turn by chipping, and consequently these surface cavities do not become an origin of fracture. In addition, it should be emphasized that the Al_2O_3/YAG eutectic composites are the materials that have a high-surface defect tolerance due to the unique cross-linked microstructure as mentioned above.

3.2. Stability at the combustion field

The burner rig test of the Al_2O_3/YAG eutectic composite resulted in crack during quenching after combustion gas exposure. The major drawback of this binary MGC material is poor property of resistance for thermal-shock, therefore, in order to apply this material to the structural application at

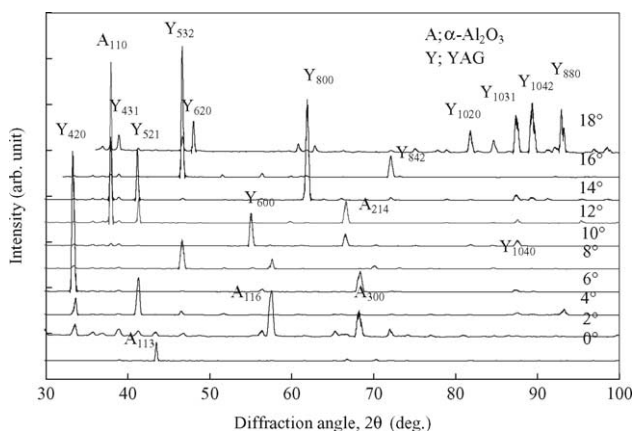


Fig. 9. XRD profiles (2θ scans, $Cu\ K\alpha$ ray) of the same corroded Al_2O_3/YAG eutectic composite after exposure wet- O_2 at $1700^\circ C$ for 200 h obtained with various incident angle (θ) of X-ray into the specimen surface (the sample was rotated keeping the incident angle). Results were unchanged compared to unexposed samples.

Table 1

Atomic fraction ratio of the sample surface as measured by XPS (at.%)	C	N	O	Na	Al	Si	S	Cl	Y
Black area	72.1	3.1	10.3	0.34	1.30	1.23	0.32	0.57	0.04
White area	41.2	3.77	33.4	1.54	12.3	1.06	–	0.80	3.66

high temperatures, the process modification is necessary as not to quench the materials at any situation.

The surface of the exposed sample was partly changed in its color in black or gray. No profile change was observed in XRD between before and after burner rig test, as well as the results of the wet- O_2 exposures. Fig. 9 shows the example of the XRD profile after the burner rig test. Only a $(hkl=1\ 1\ 3)$ reflection of $\alpha-Al_2O_3$ phase was observed at $2\theta=0$ in the figure. With inclining the surface of the sample, few reflections (or single-family reflections like Fig. 9) of $\alpha-Al_2O_3$ or YAG appeared, except for the cases that there are two or more lattice planes with similar face-angles, these indicating being single crystal phases.

The comparison of the atomic fraction of the elements between the color-changed part and color-unchanged parts analyzed by XPS is summarized in Table 1. Carbon was detected from both parts of the sample, and its concentration of

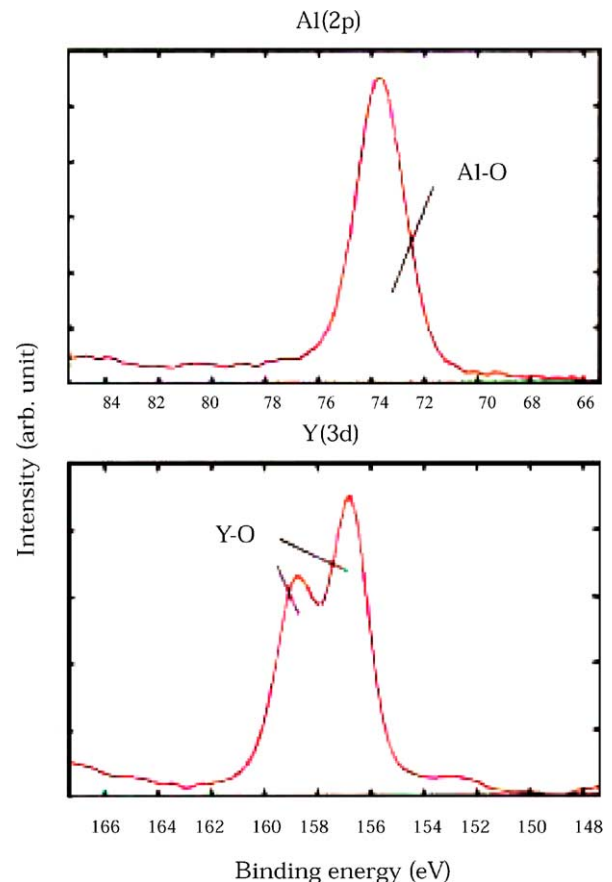


Fig. 10. XPS spectra of $Al(2p)$ and $Y(3d)$ of the same sample as that in Table 1 (black area).

the color-changed part was higher than the other one. This indicates that the XPS peak of the carbon is due to the formation of soot during fuel-rich combustion.

Fig. 10 shows XPS spectra of Al(2p) and Y(3d) of this sample surface. It is clearly seen, that the Al and Y elements chemically bonded to oxygen, and there is not seen any other bonding. Therefore, the cause of the color-change at the surface of the sample was attached soot. It is concluded that Al₂O₃ and YAG are stable even in the fuel-rich combustion gas at 1500 °C.

4. Conclusion

The stability of the Al₂O₃/YAG eutectic composite in wet-O₂ vapor (50% O₂/50% H₂O) has been examined at 1700 °C for 200 h. The presence of water vapor slightly affected the weight and volume of the sample of this material. The surface morphology change due to the thermal swelling and chipping was rarely observed after the exposure. The evaluation of the fracture strength of the corroded sample indicates that the mechanical strength was not affected by the corrosion by water vapor at 1700 °C for 200 h. Despite the changes in surface morphology and density, the Al₂O₃/YAG eutectic composite maintain the original flexural strength and show good corrosion resistance.

Acknowledgment

The authors are grateful to Dr. Ali Sayir of John H. Glenn Research Center at Lewis Field for his beneficial discussion on volatilization of Al₂O₃ in wet atmosphere at elevated temperatures.

References

1. Lange, F. F., Relation between strength, fracture energy, and microstructure of hot-pressed Si₃N₄. *J. Am. Ceram. Soc.*, 1973, **56**(10), 518–522.
2. Song, H. and Coble, R. L., Origin and growth kinetics of platelike abnormal grains in liquid-phase-sintered alumina. *J. Am. Ceram. Soc.*, 1990, **73**(7), 2077–2085.
3. Ismail, M. G. M. U., Nakai, Z. and Somya, S., Microstructure and mechanical properties of mullite prepared by the sol-gel method. *J. Am. Ceram. Soc.*, 1987, **70**, C-7–C-8.
4. Katz, R. N., Grendahl, S., Cho, K., Bar-On, I. and Rafaniello, W., Fracture toughness of ceramics in the AlN-SiC system. *Ceram. Sci. Eng. Proceed.*, 1994, **15**(5), 877–884.
5. Waku, Y., Ohtsubo, N., Nakagawa, N. and Kohtoku, Y., Sapphire matrix composites reinforced with single crystal YAG phases. *J. Mater. Sci.*, 1996, **31**, 4463–4670.
6. Waku, Y., Nakagawa, N., Wakamoto, T., Otsubo, H., Shimizu, K. and Kohtoku, Y., The creep and thermal stability characteristics of a unidirectionally solidified Al₂O₃/YAG eutectic composite. *J. Mater. Sci.*, 1998, **33**, 4943–4951.
7. Otsuka, A., Waku, Y. M., Kitagawa, K. and Arai, N., Effect of hot corrosive environment on ceramics. *Energy*, 2005, **30**(2–4), 523–533.
8. Opila, E. J. and Myers, D. L., Alumina volatility in water vapor at elevated temperature. *High Temp. Mater. Chem. IV: Electrochem. Soc. Proc.*, 2003, **16**, 535–544.
9. Opila, E. J. and Jacobson, N. S., Volatile hydroxide species of common protective oxides and their role in high temperature corrosion. *Proc. Electrochem. Soc.*, 1997, **96**(26), 269–280.
10. Tai, W. and Watanabe, T., Elevated-temperature toughness and hardness of a hot-pressed Al₂O₃-WC-Co composite. *J. Am. Ceram. Soc.*, 1999, **82**(1), 245–248.
11. Yue, X., Zhang, G., Watanabe, T. and Tai, W., Corrosion behavior of single-crystal alumina in argon, air, and water vapor atmospheres at 1700–2000 °C. *J. Am. Ceram. Soc.*, 1999, **82**(9), 2560–2562.
12. Bahlawane, N., Watanabe, T., Waku, Y., Mitani, A. and Nakagawa, N., Effect of moisture on the high-temperature stability of unidirectionally solidified Al₂O₃/YAG eutectic composites. *J. Am. Ceram. Soc.*, 2000, **83**(12), 3077–3081.